Stanford Exploration Project, Report 97, July 8, 1998, pages 217–241

Stanford Exploration Project, Report 97, July 8, 1998, pages 217–241

The offset-midpoint traveltime pyramid in transversely isotropic media

Tariq Alkhalifah[1]

keywords: *anisotropy, traveltimes*

ABSTRACT

Prestack Kirchhoff time migration, for transversely isotropic media with a vertical symmetry axis (VTI media), is implemented using an offset-midpoint traveltime equation; Cheop's pyramid equation for VTI media. The derivation of such an equation required approximations that pertain to high frequency and weak anisotropy. Yet, the resultant offset-midpoint traveltime equation for VTI media is highly accurate for even strong anisotropy. It is also strictly dependent on two parameters: the normal-moveout (NMO) velocity and the anisotropy parameter, η. It reduces to the exact offset-midpoint traveltime equation for isotropic media when $\eta = 0$. In vertically inhomogeneous media, the NMO velocity and η parameters in offset-midpoint traveltime equation are replaced by their effective values; the velocity is replaced by the root-mean-squared velocity, whereas η is given by a more complicated equation that includes summation of the fourth power of velocity.

INTRODUCTION

Analytical representation of traveltime equations is necessary for efficient velocity estimation. For isotropic media, traveltimes as a function of offset and common midpoint (CMP) are given by a simple analytical equation [the double-square-root equation (DSR)] in homogeneous media (Yilmaz and Claerbout, 1980). In vertically inhomogeneous media, the velocity in this analytical equation is replaced by its root-mean-squared (RMS) average velocity. The DSR equation is often used to implement efficient prestack time migration (Karrenback and Gardner, 1988; Bancroft and Geiger, 1994); the kind that can be used for iterative velocity estimation.

However, velocities estimated based on the isotropic assumption have seldom provided us with the full story; seismic depth mis-ties with well logs, among other shortcomings, have resulted from such a medium restriction. Some of these shortcomings can be attributed to the presence of complicated lateral velocity variations, however,

[1]**email:** tariq@sep.stanford.edu

many can only be explained by the presence of anisotropy (Banik, 1984).

Since no analytical relation between the group velocity and ray angle exists, traveltimes in transversely isotropic media with a vertical symmetry axis (VTI media), even for the homogeneous case, are often calculated numerically (Richards, 1960). Such a limitation has restricted parameter estimation in VTI media, especially with regard to using prestack time migration. Equations for anisotropic media are better represented using plane waves, with phase velocities that can be described analytically as a function of propagation direction. Efficient treatment of plane waves, however, is only possible in the Fourier domain. The main drawback of this domain is the loss of the lateral position information, and so the Fourier domain cannot efficiently treat media with lateral inhomogeneity. With stationary phase approximations (Alkhalifah, 1997b), we can, however, obtain analytical representations of traveltime in the space-time domain from the well-known analytical equations in the Fourier domain.

In this paper, I derive approximate analytical equations that describe traveltime as a function of offset and midpoint in VTI media. Though an approximation, its accuracy far exceeds any previous representations, even for the case of horizontal reflections. This equation, Cheop's pyramid for VTI media, will be used to implement efficient space-time domain Kirchhoff time migration. For vertically inhomogeneous media, average equivalent velocities and anisotropic parameters are used in the analytical equation. The accuracy of these equations are demonstrated on synthetic data.

ANISOTROPIC MEDIA PARAMETERIZATION

Here, I consider the simplest and probably most practical anisotropic model, that is, a transversely isotropic (TI) medium with a vertical symmetry axis. Although more complicated kinds of anisotropies can exist (i.e., orthrohombic anisotropy), the large amount of shales present in the subsurface implies that the TI model has the most influence on P-wave data (Banik, 1984).

In homogeneous transversely isotropic media with a vertical symmetry axis (VTI media), P- and SV-waves[2] can be described by the vertical velocities V_{P0} and V_{S0} of P- and S-waves, respectively, and two dimensionless parameters ϵ and δ (Thomsen, 1986).

$$\epsilon \equiv \frac{c_{11} - c_{33}}{2c_{33}},$$

$$\delta \equiv \frac{(c_{13} + c_{44})^2 - (c_{33} - c_{44})^2}{2c_{33}(c_{33} - c_{44})}.$$

Alkhalifah (1997a) demonstrated that P-wave velocity and traveltime are practically independent of V_{S0}, even for strong anisotropy. This implies that, for practical pur-

[2]I omit the qualifiers in "quasi-P-wave" and "quasi-SV-wave" for brevity

poses, P-wave kinematic signatures is a function of just three parameters: V_{P0}, δ, and ϵ.

Alkhalifah and Tsvankin (1995) further demonstrated that a new representation in terms of just *two* parameters is sufficient for performing all time-related processing, such as normal moveout correction (including non-hyperbolic moveout correction, if necessary), dip-moveout correction, and prestack and post-stack time migration. These two parameters are the normal-moveout velocity for a horizontal reflector

$$V_{\mathrm{nmo}}(0) = V_{p0}\sqrt{1+2\delta}\,, \tag{1}$$

and the anisotropy coefficient η,

$$\eta \equiv \frac{1}{2}\left(\frac{V_h^2}{V_{\mathrm{nmo}}^2(0)} - 1\right) = \frac{\epsilon-\delta}{1+2\delta}\,, \tag{2}$$

where V_h is the horizontal velocity. Instead of V_{nmo}, I will use v to represent the interval NMO velocity in both isotropic and TI media. The midpoint-offset traveltime equations, like any other time-domain equations, are expected to be dependent on these to parameters as well.

THE MIDPOINT-OFFSET TRAVELTIME EQUATION

To derive an analytical prestack-migration traveltime equation in the space-time domain, I will start by casting the prestack migration in the Fourier (frequency-wavenumber) domain, where the traveltime shifts are described analytically. Such a migration is commonly referred to as phase-shift migration (Gazdag, 1978; Yilmaz, 1979). The prestack version of this migration for anisotropic media is described in detail by Alkhalifah (1997b).

Prestack phase-shift migration

The Phase-shift operator in a prestack Fourier-domain is described by the double-square-root equation, which is a function of the angular frequency ω, the midpoint rayparameter p_x, the offset rayparameter p_h, and the velocity, v. Constant-velocity prestack migration, with output provided in two-way vertical time (τ), in offset-midpoint coordinates (Yilmaz, 1979), is given by:

$$g(t=0,k_x,h=0,\tau) = \int d\omega \int dk_h\; e^{i\omega\tilde{p}_\tau(p_x,p_h)\tau} F(\omega,k_x,k_h,\tau=0), \tag{3}$$

where $F(\omega,k_x,k_h,\tau=0)$ is the 3-D Fourier transform of the field $f(t,y,h,\tau=0)$ recorded at the surface, given by

$$F(\omega,k_x,k_h,\tau=0) = \int dt\; e^{-i\omega t} \int dy e^{ik_x x} \int dh e^{ik_h h} f(t,x,h,\tau=0),$$

and $k_x = 2\omega p_x$, $k_h = 2\omega p_h$, and $k_z = 2\frac{\omega}{v} p_\tau$ are the horizontal midpoint wavenumber, the horizontal offset wavenumber, and the vertical wavenumber, respectively. In this paper, I will freely alternate between the half offset, h, and the full offset, X, in representing the offset axis, where $X = 2h$. The phase factor $\tilde{p}_\tau(p_x, p_h)$, for isotropic media, is defined as

$$\tilde{p}_\tau(p_x, p_h) \equiv \frac{1}{2}(\left[1 - v^2(p_x + p_h)^2\right]^{\frac{1}{2}} + \left[1 - v^2(p_x - p_h)^2\right]^{\frac{1}{2}}), \tag{4}$$

which is a normalized version of the double-square-root (DSR) equation. The two integrals in ω and k_h in equation (3) represent the imaging condition for zero offset and zero time ($h = 0, t = 0$).

For VTI media, the phase factor is given by a more complicated equation Alkhalifah (1997b),

$$\tilde{p}_\tau(p_x, p_h) \equiv \frac{1}{2}\left(\sqrt{1 - \frac{(p_x + p_h)^2 v^2}{1 - 2\eta v^2 (p_x + p_h)^2}} + \sqrt{1 - \frac{(p_x - p_h)^2 v^2}{1 - 2\eta v^2 (p_x - p_h)^2}}\right). \tag{5}$$

The dispersion equation, now, includes η as well as the velocity.

Kirchhoff migration is typically applied by smearing an input trace, after the proper traveltime shifts, over the output section in a summation process. To obtain the response of inserting a single trace into the prestack phase-shift migration [equation (3)], we multiply the input data by a Direc-delta function in midpoint and offset axes as follows

$$f(t, x, h, \tau = 0) = \tilde{f}(t, x, h, \tau = 0)\delta(x - x_0, h - h_0), \tag{6}$$

where x_0 is the midpoint location and h_0 is the offset of the input trace. The Fourier transform of equation (6) is given by

$$F(\omega, k_x, k_h, \tau = 0) = \tilde{F}(\omega, x_0, h_0, \tau = 0) e^{ik_x x_0 + ik_h h_0}.$$

Inserting this equation into equation (3) provides us with the migration response to a single input trace given by

$$g(t = 0, x, h = 0, \tau) = \int d\omega \tilde{F}(\omega, x_0, h_0, \tau = 0) \int dk_h \int dk_x \, e^{i\omega T}, \tag{7}$$

where the new phase shift function is given by

$$T = \frac{1}{2}\left(\sqrt{1 - \frac{(p_x + p_h)^2 v^2}{1 - 2\eta v^2 (p_x + p_h)^2}} + \sqrt{1 - \frac{(p_x - p_h)^2 v^2}{1 - 2\eta v^2 (p_x - p_h)^2}}\right)\tau + 2p_x(x - x_0) + 2p_h h_0. \tag{8}$$

The number of integrals in Equation (7) can be reduced by recognizing areas in the integrand that contribute the most to the integrals in k_h and k_x. Since the integrand is an oscillatory function its biggest contributions take place when the oscillations are stationary, when the phase function is either minimum or maximum. This approach is referred to as the stationary phase method (Appendix C). The stationary points (p_x and p_h) correspond to the minimum or maximum of equation (8). In fact, the phase has a dome-like shape as a function of p_x and p_h (see Figure 1). Thus, to calculate the stationary points, we must set the derivative of equation (8) with respect to p_h and p_x to zero, and solve the two equations for these two parameters. An easier approach is discussed next and in Appendix A.

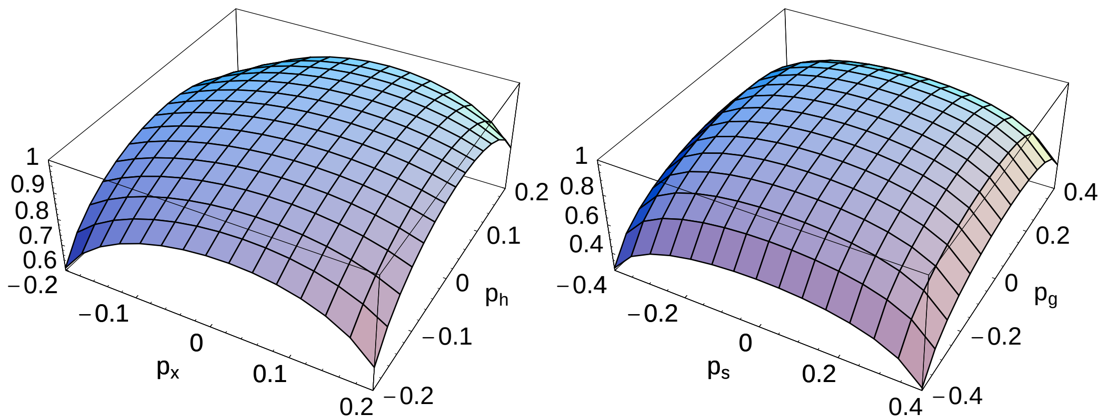

Figure 1: Traveltime, in seconds, as a function offset-midpoint rayparameters (left), and source-receiver rayparameters (right) computed using equation (8). All rayparameters have units of s/km. In both plots, the midpoint shift $x - x_0 = 0.1$ km, the offset is 0.2 km, and vertical time of 1 s. The medium parameters considered are v=2 km/s, $\eta = 0.2$. tariq3-station [NR]

Cheop's pyramid for VTI media

To find the maximum of equation (8), we take its derivative with respect to p_h and p_x, and set these derivatives to zero. The stationary point along the p_h-p_x plane is obtained by solving the two new nonlinear equations in terms of p_x and p_h. Since the source rayparameter, p_s, and the receiver rayparameter, p_g, are linearly related to p_x and p_h, as follows

$$p_s = p_x - p_h,$$

and

$$p_g = p_x + p_h,$$

we can find the stationary point solution by solving for p_s and p_g, instead of solving for p_x and p_h. Solving for p_s and p_g yields two independent nonlinear equations corresponding to the source and receiver rays, that can be solved separately.

The stationary point solutions (Appendix A) are then given by

$$p^2 = \frac{y^2\,\left(y^6 + 6\,v^2\,y^4\,(1-\eta)\,\tau^2 + 3\,v^4\,y^2\,(3+4\,\eta)\,\tau^4 + 4\,v^6\,\tau^6\right)}{v^2\,\left(y^2 + v^2\,\tau^2\right)\,\left(y^6\,(1+2\,\eta) + 2\,v^2\,y^4\,(3+5\,\eta)\,\tau^2 + v^4\,y^2\,(9+44\,\eta)\,\tau^4 + 4\,v^6\,\tau^6\right)}, \tag{9}$$

where y is either the lateral distance between the image point and source, given by $2(x-x_0-h)$ for p_s, or the lateral distance between the image point and receiver, given by $2(x-x_0+h)$ for p_g.

For isotropic media, $\eta = 0$ and equation (9) reduces to

$$p_{\rm is}^2 = \frac{y^2}{v^2\,y^2 + v^4\,\tau^2}, \tag{10}$$

where

$$\sin^2\theta = \frac{y^2}{y^2 + v^2\,\tau^2}, \tag{11}$$

and

$$p_{\rm is} = \frac{\sin\theta}{v}.$$

As a result,

$$p^2 = p_{\rm is}^2\,\frac{\left(y^6 + 6\,v^2\,y^4\,(1-\eta)\,\tau^2 + 3\,v^4\,y^2\,(3+4\,\eta)\,\tau^4 + 4\,v^6\,\tau^6\right)}{\left(y^6\,(1+2\,\eta) + 2\,v^2\,y^4\,(3+5\,\eta)\,\tau^2 + v^4\,y^2\,(9+44\,\eta)\,\tau^4 + 4\,v^6\,\tau^6\right)}, \tag{12}$$

For traveltime calculation, equation (9) for p_s and p_g is inserted into

$$t(\tau,x,h,v,\eta) = \frac{\tau}{2}\left(\sqrt{1-\frac{v^2\,{p_g}^2}{1-2\,v^2\,\eta\,{p_g}^2}} + \sqrt{1-\frac{v^2\,{p_s}^2}{1-2\,v^2\,\eta\,{p_s}^2}}\right) + 2\,p_g\,y_g + 2\,p_s\,y_s, \tag{13}$$

where $y_s = 2(h-x+x_0)$ and $y_g = 2(h+x-x_0)$.

Equation (13) is the offset-midpoint (Cheop's pyramid) equation for VTI media. The derivation included the stationary phase (high frequency) approximation, as well as approximations corresponding to small η. For η=0, equation (13) reduces to the exact form (high-frequency limit) for isotropic media. However, for large η the equation, as we will see later, is extremely accurate. Figure 2 shows the traveltime calculated using equation (13) as a function of offset and midpoint for three η values. The shape of the traveltime function resembles Cheop's pyramid, and as a result was given the name. Unlike the isotropic medium pyramid, the VTI ones include nonhyperbolic moveout along the offset and midpoint axis. Clearly, the higher horizontal velocity in the VTI media resulted in faster traveltime with increasing offset and midpoint than the isotropic case.

The stationary phase method also provides an amplitude factor given by the second derivative of the phase function [equation (8)] with respect to p_s and p_g. Specifically, the amplitude is proportional to the reciprocal of the square root of the second derivative of the phase evaluated at the stationary point (Appendix C).

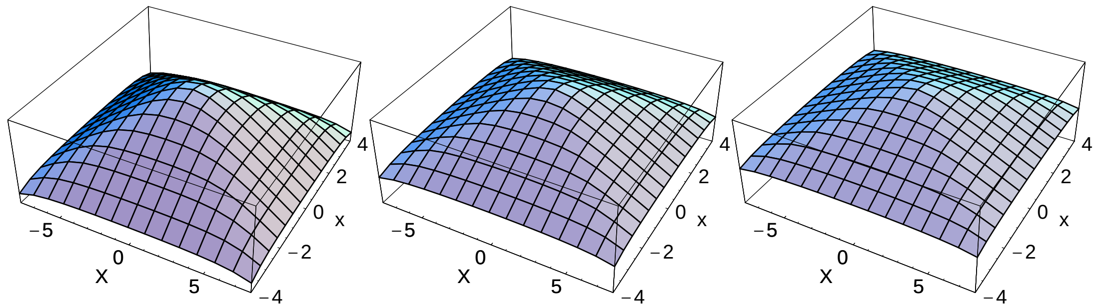

Figure 2: Traveltime, in seconds, as a function offset, X, and midpoint, x, both in km, for, from left to right, an isotropic media ($\eta = 0$), a VTI media with $\eta = 0.2$, and a VTI media with $\eta = 0.4$, respectively. The velocity is 2 km/s and the vertical time is 1 s, for all three pyramids. tariq3-pyr3 [NR]

VERTICAL VELOCITY VARIATION

In vertically inhomogeneous media, traveltimes can be calculated numerically using any standard numerical technique. Alternatively, traveltimes in $v(z)$ media can be approximated using the homogeneous-medium equations [i.e., equation (13)] with replacing the medium parameters by their effective values.

First, as usual, the normal-moveout velocity involves a root-mean-squared average of velocities in the previous layers. Specifically

$$V^2(\tau) = \frac{1}{\tau} \int_0^{\tau} v^2(t)dt, \tag{14}$$

where all lower-case variables V correspond to interval-velocity values, and all upper-case variables V correspond to RMS averaged values.

From Appendix B, the anisotropy parameterη in equations (12) and (13), is replaced by

$$\eta_{\text{eff}}(\tau) = \frac{1}{8}\{\frac{1}{t_0 V^4(\tau)} \int_0^{\tau} v^4(t)[1 + 8\eta(t)]dt - 1\}, \tag{15}$$

which includes a summation over the fourth power in velocity. These two equations are similar to what Alkhalifah (1997) used for his nonhyperbolic analysis. Thus, now it is safe to say that such averaging holds for dipping events as well since equation (13) handles dipping events. However, for dipping events the effective values are computed along the zero-offset ray. In $v(z)$ media, the effective values for dipping and horizontal reflectors are the same. The difference appears only when lateral inhomogeneity exists.

3-D MEDIA

In 3-D media, the rayparameters for each of the sources and receivers have two components: p_x and p_y. For general anisotropic media, this suggests that we need to solve for two parameters for each of the source and receiver rays in resolving a 2-D stationary point problem. This results in a fairly complicated process that can be avoided by relying on polar coordinates.

In VTI media, unlike more complicated anisotropies, the group and phase angles for a given ray are confined to the same vertical plane that includes the source or the receiver and the image point. Simply stated, the VTI model with respect to the horizontal plane is isotropic. We can simplify the 3-D problem by using azimuth instead of multi-component rayparameters. As a result, only one parameter need to be solved for each of the source and receiver rays, and this rayparameter has the same form given in the 2-D case [equation (12)].

The four stationary points in 3-D media are:

$$p_{sx} = p_s \cos\phi_s, \quad p_{sy} = p_s \sin\phi_s,$$

$$p_{gx} = p_g \cos\phi_g, \quad p_{gy} = p_g \sin\phi_g,$$

where ϕ_s and ϕ_g is the source-to-image-point and receiver-to-image-point azimuth, respectively. The polar rayparameters (p_s and p_g) are computed using equation (12) with

$$y = 2\sqrt{(h + (x - x_0))^2 + (y - y_0)^2}$$

for p_g, and

$$y = 2\sqrt{(h - (x - x_0))^2 + (y - y_0)^2}$$

for p_s.

Therefore, the total traveltime is given by

$$t(\tau, x, h, v, \eta) = \frac{\tau}{2}\left(\sqrt{1 - \frac{v^2\, {p_g}^2}{1 - 2\, v^2\, \eta\, {p_g}^2}} + \sqrt{1 - \frac{v^2\, {p_s}^2}{1 - 2\, v^2\, \eta\, {p_s}^2}}\right) + 2\, p_g\, y_g + 2\, p_s\, y_s, \tag{16}$$

where $y_s = 2\sqrt{(h - (x - x_0))^2 + (y - y_0)^2}$, and $y_g = 2\sqrt{(h + (x - x_0))^2 + (y - y_0)^2}$. Equation (16) can be used to perform prestack time migration on 3-D datasets.

THE ACCURACY OF THE VTI EQUATION FOR HORIZONTAL REFLECTORS

Setting $x - x_0 = 0$ in the offset-midpoint traveltime equation yields a formula that describes the moveout of reflections from horizontal reflectors. Since many of these moveout equations exist (Hake et al., 1984; Tsvankin and Thomsen, 1994), I will compare the offset axis of our VTI offset-midpoint traveltime equation with these equations, as well as with the exact solution computed numerically. Specifically, I will measure the difference in traveltimes between the various moveout approximations and the numerically computed solution. This difference is given in terms of the percentage error in traveltime as a function of offset. Clearly all approximations yield the exact solution for zero-offset, since they are derived based on this limit.

For a horizontal reflector $x - x_0 = 0$, as well as $p_x = 0$, in equations (12) and (13), and thus they reduce to

$$T(\tau, h, v, \eta) = 2\,h\,p_h + \tau\,\sqrt{1 - \frac{v^2\,{p_h}^2}{1 - 2\,v^2\,\eta\,{p_h}^2}}, \tag{17}$$

where

$$p_h = \frac{X^2\,\left(X^6 - 6\,X^4\,v^2\,(-1+\eta)\,\tau^2 + 3\,X^2\,v^4\,(3+4\,\eta)\,\tau^4 + 4\,v^6\,\tau^6\right)}{v^2\,\left(X^2 + v^2\,\tau^2\right)\left(X^6\,(1+2\,\eta) + 2\,X^4\,v^2\,(3+5\,\eta)\,\tau^2 + X^2\,v^4\,(9+44\,\eta)\,\tau^4 + 4\,v^6\,\tau^6\right)},$$

and X is the offset.

Hake et al. (1984) derived a three-term Taylor series expansion for the moveout of reflections from horizontal interfaces in homogeneous, VTI media. Their traveltime equation can be simplified when expressed in terms of η and v (Alkhalifah and Tsvankin, 1995), as follows:

$$t^2(X) = \tau^2 + \frac{X^2}{v^2} - \frac{2\eta X^4}{t_0^2 v^4}. \tag{18}$$

The first two terms on the right correspond to the hyperbolic portion of the moveout, whereas the third term approximates the nonhyperbolic contribution. Note that the third term (fourth-order in X) is proportional to the anisotropy parameter η, which therefore controls nonhyperbolic moveout directly.

Tsvankin and Thomsen (1994) derived a correction factor to the nonhyperbolic term of Hake et al's (1984) equation that increases the accuracy and stabilizes traveltime moveout at large offsets in VTI media. The more accurate moveout equation, when expressed in terms of η and v (Alkhalifah and Tsvankin, 1995), and slightly manipulated, is given by

$$t^2(X) = \tau^2 + \frac{X^2}{v^2} - \frac{2\eta X^4}{v^2[t_0^2 v^2 + (1+2\eta)X^2]}. \tag{19}$$

Figure 3 shows the percentage error in traveltime moveout as a function of offset for the three moveout equations given above. Clearly, the offset-axis component of the new VTI pyramid equation (dashed gray curve) has less errors and is by far more accurate than the traveltime moveout given by either the three-term Taylors series equation (18) (solid gray curve) or the modified traveltime moveout equation (19)

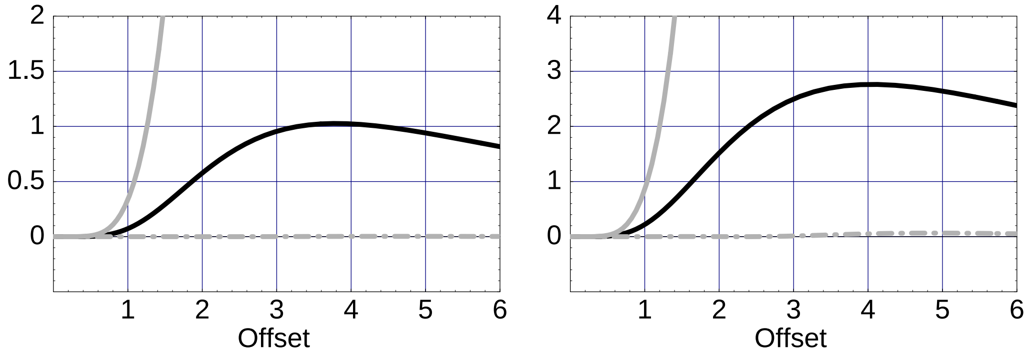

Figure 3: Percentage errors in traveltime moveout from a horizontal reflector as a function of offset. The solid gray curve corresponds to using Hake et al's equation (18), the solid black curve corresponds to using equation (19), and the dashed gray curve corresponds to using our new equation (17). The medium is VTI with $\eta = 0.2$ (left), and $\eta = 0.4$ (right). The velocity is 2 km/s and the vertical traveltime is 2 s. tariq3-Error2eta [NR]

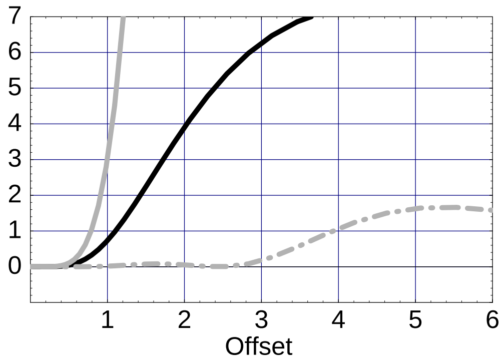

Figure 4: Same as Figure 3, but with $\eta = 1.0$, which is an extremely high value for η, not common in the subsurface. tariq3-Erroreta1 [NR]

(solid black curve). In fact, the errors in equation (17) for moderate anisotropy, given by $\eta = 0.2$ (left), and relatively strong anisotropy, given by $\eta = 0.4$ (right), are practically zero for offsets-to-depth ratio up to 3, shown here. We have to use a model with η equals the huge value of 1, as shown in Figure 4, before observing any sizable errors in the new equation. Even for such a huge anisotropy, the errors are again practically zero for offsets-to-depth ratio below 1.5. Therefore, for all intent and purposes in seismic applications, equation (8) for horizontal reflectors is practically exact. Next, we test the accuracy of the midpoint-offset pyramid equation for dipping reflectors. We do that by prestack migrating synthetic data that include dipping reflections using this new equation.

SYNTHETIC EXAMPLES

The midpoint-offset traveltime equation [equation (13)] can be used directly in a prestack Kirchhoff-type migration of common-offset gathers. This equation provides us with the summation curve used to implement the Kirchhoff migration for a given offset. Using such a prestack migration, I will test the accuracy of equation (13) by migrating synthetic data that include horizontal, as well as dipping, reflections. The position of the migrated reflectors as well as the moveout after migration are two key indicators to the accuracy of the new pyramid equation for VTI media. The synthetic data are generated using a method described by Alkhalifah (1995) for VTI media. The test here is applied to homogeneous, as well as $v(z)$ media.

Homogeneous media

For the homogeneous medium case, I will use the reflector model shown in Figure 5, which includes a syncline structure with flanks dipping at about 50 degrees. Since we are forced to have a finite aperture coverage, it will be hard to migrate large dip angles in a homogeneous medium. Another dipping event at a shallower depth is also included in the model.

The synthetic seismograms are generated considering a VTI medium with velocity of 2 km/s and a realistic η of 0.3. Figure 6 shows four synthetic seismograms generated using the model in Figure 5 for offsets of (a) 0, (b) 1, (c) 2, and (d) 3 km. The limited recording aperture has cut off some of the energy of the reflection from the right flank of the syncline. As a result, the right flank is expected to be weaker after migration, due to the missing energy. Also, the appearance of under migration usually accompanies dipping reflections that have not been totally recorded at the surface.

Figure 7 shows the prestack time migration of the synthetic data given in Figure 6 for, again, an offset of (a) 0, (b) 1, (c) 2, and (d) 3 km. All the migrated sections for the various offsets seem accurate and the reflections are well positioned. One way to test the accuracy of the migrated sections is to convert them to depth and overlay the depth model in Figure 5 over these migrated sections. Figure 8 shows

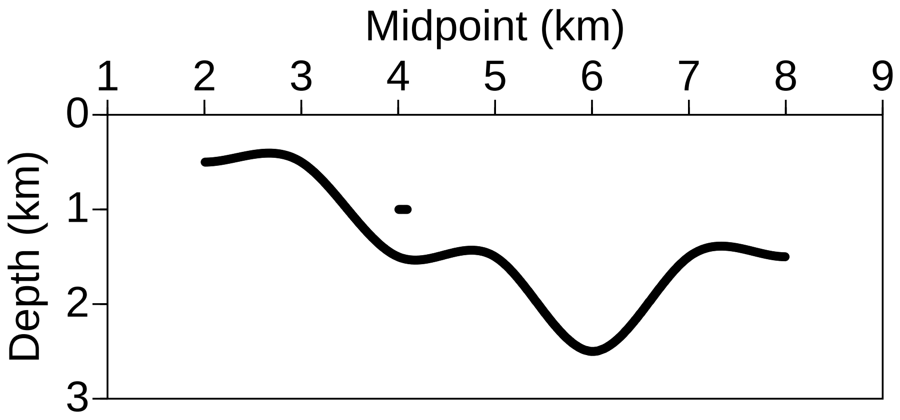

Figure 5: A simple reflector with a syncline structure in the middle embedded in a homogeneous transversely isotropic model with $v = 2.0$ km/s and $\eta = 0.3$. tariq3-modelsm [NR]

the migrated sections in depth, converted using the velocity of 2 km/s, from top to bottom having offsets of 0, 1, 2, and 3 km, respectively. All migrated sections agree well with the model used to generate the synthetic seismograms. Since the synthetic seismograms were generated using exact (within the limit of ray theory) traveltimes, the accuracy of the migration is attributable to the accuracy of the midpoint-offset traveltime equation, derived in this paper. Again, an appearance of under migration of the right flank of the syncline is the result of the limited recording aperture, that has cut of some the energy associated with this flank.

Looking at the moveout of the dipping events after migration, shown in Figure 9, clearly demonstrates the accuracy of the midpoint-offset traveltime equation for dipping events. Therefore, any moveout misalignment can only be attributable to inaccurate medium parameters used in the migration, not the equation used.

Vertically inhomogeneous media

For the $v(z)$ medium case, I will use the reflector model shown in Figure 10, which includes reflectors with dips ranging from 0 to 90 degrees. In $v(z)$ media, unlike in homogeneous media, dips up to and beyond 90 degrees can be recorded with a limited aperture due to the ray bending. However, since our equation is based on the equivalent medium assumption some of the restrictions of the homogeneous case will hold in the $v(z)$ approximation as well.

Figure 11 shows four synthetic seismograms generated using the model in Figure 10

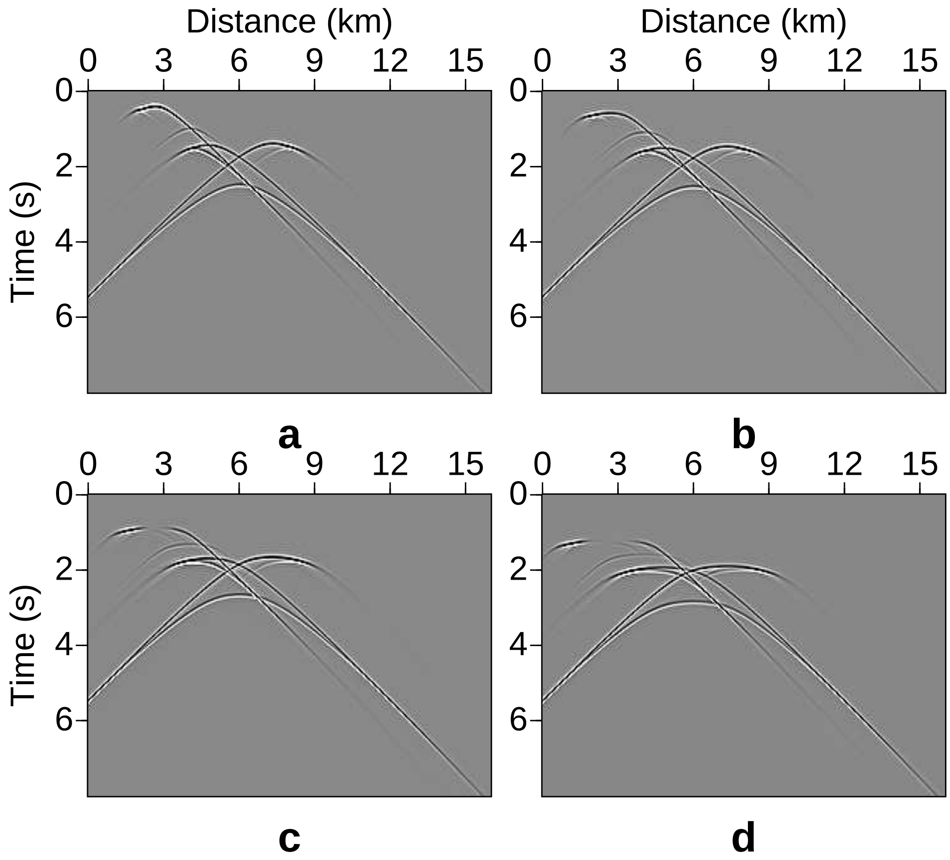

Figure 6: Synthetic seismograms for the model in Figure 5 for (a) coincident source and receiver (zero-offset), (b) an offset of 1 km, (c) an offset of 2 km, and (d) an offset of 3 km. tariq3-synh [NR]

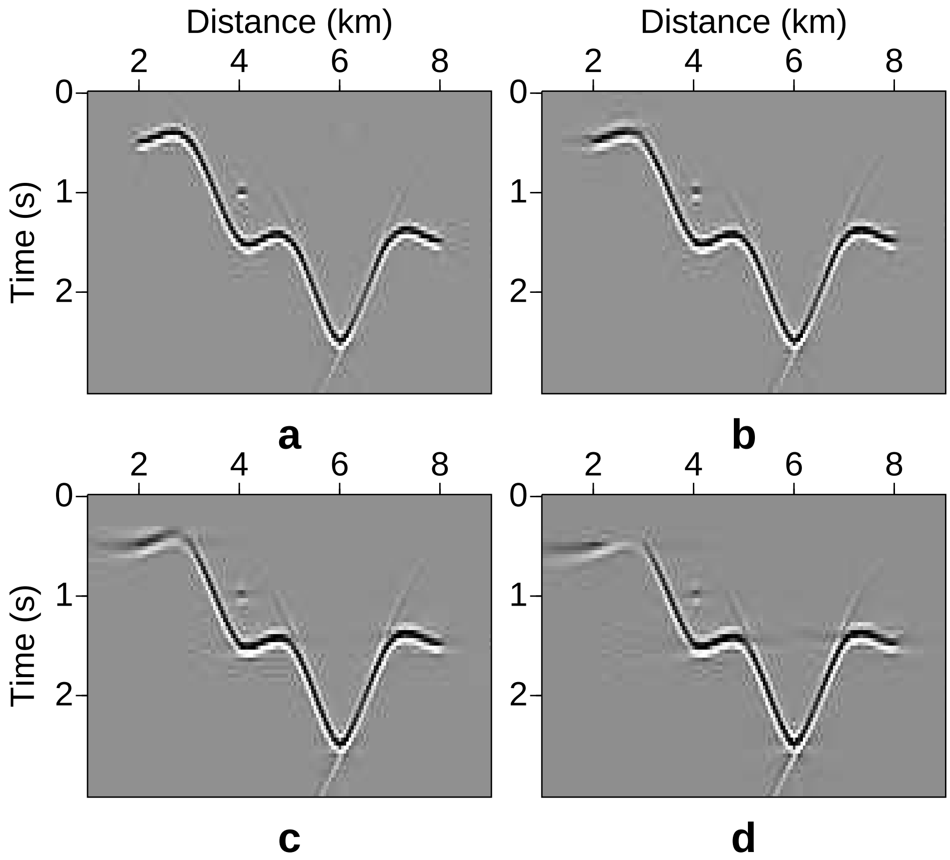

Figure 7: Prestack time migration of the synthetic seismograms shown in Figure 6, again, for (a) zero-offset, (b) offset of 1 km, (c) offset of 2 km, and (d) offset of 3 km. The lower energy of the right flank of the syncline is the result of the limited aperture. tariq3-migh [NR]

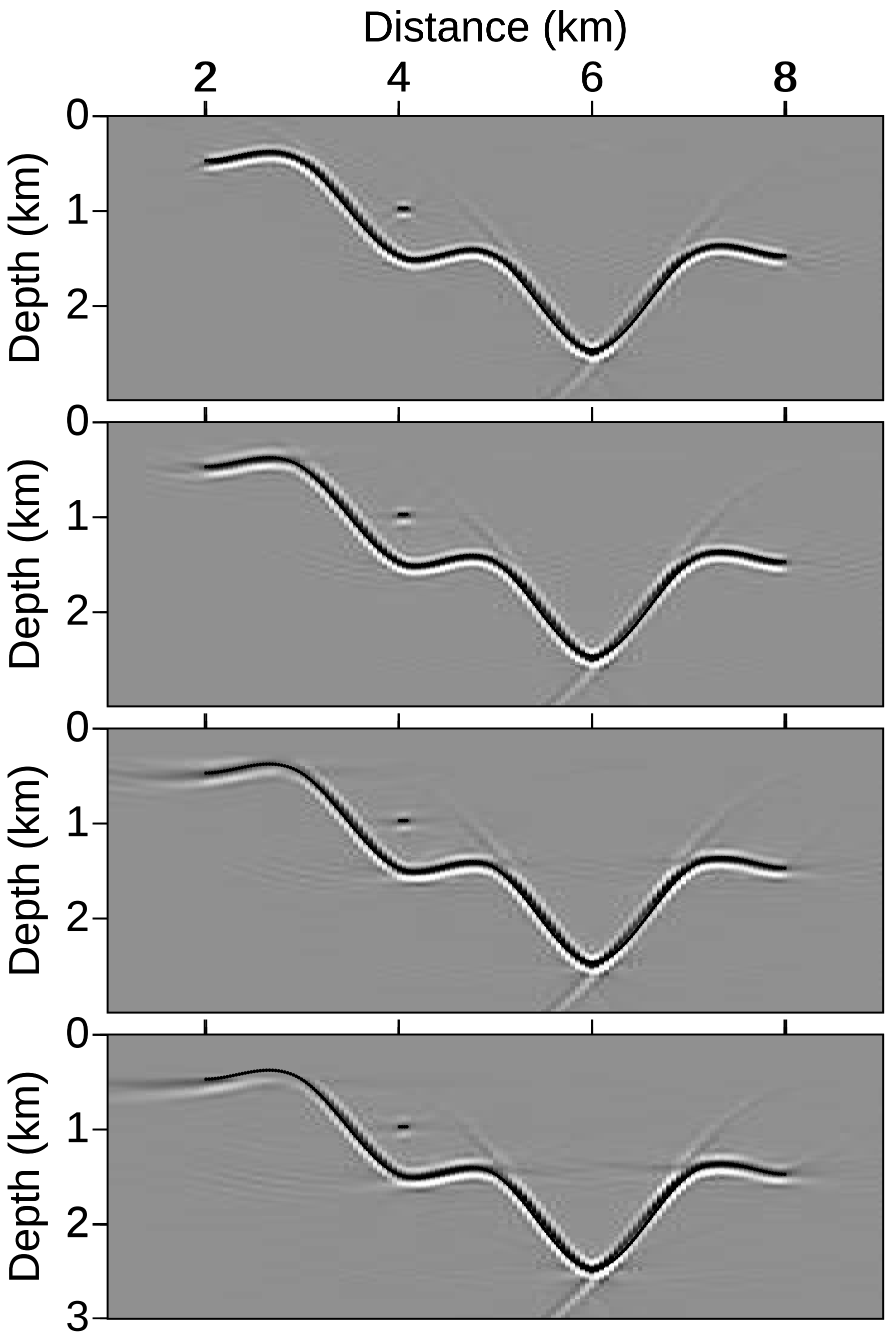

Figure 8: The time migrated sections converted to depth for an offset, from top to bottom, of zero, 1, 2, and 3 km, respectively. The reflector shape in Figure 5 is overlaid on the migration results. tariq3-mighm [NR]

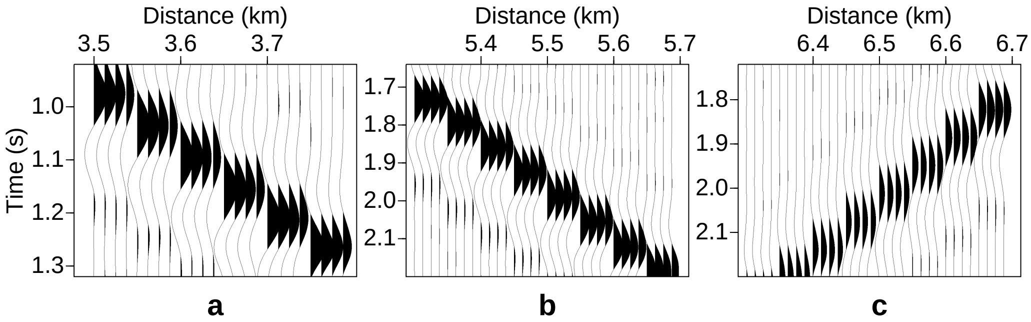

Figure 9: Detail wiggle plots of the migrated sections sorted in common gather format, where the different offsets. are plotted next to each other. $\boxed{\text{tariq3-migoff2}}$ [NR]

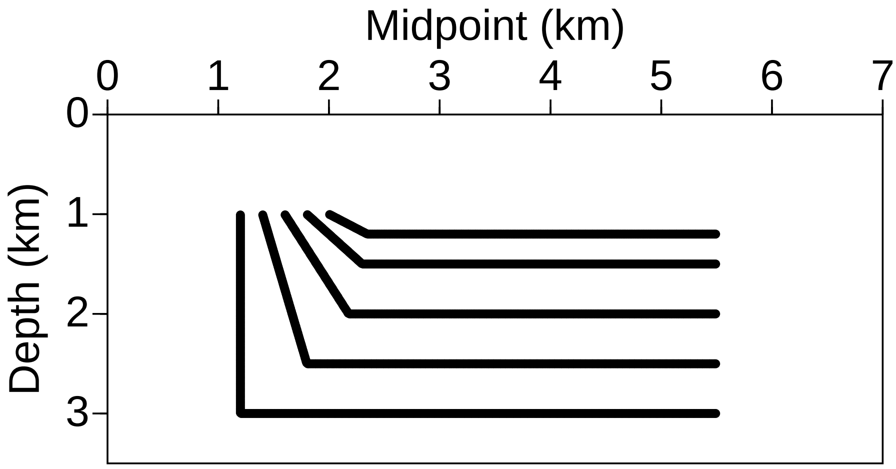

Figure 10: A reflector model consisting of reflectors dipping at 0, 30, 45, 60, 75, and 90 degrees in a $v(z)$ transversely isotropic model with $v = 1.5 + 0.6z$ km/s and $\eta = 0.2$. $\boxed{\text{tariq3-modelvz}}$ [NR]

for offsets of (a) 0, (b) 1, (c) 2, and (d) 3 km. Figure 12 shows prestack time migration

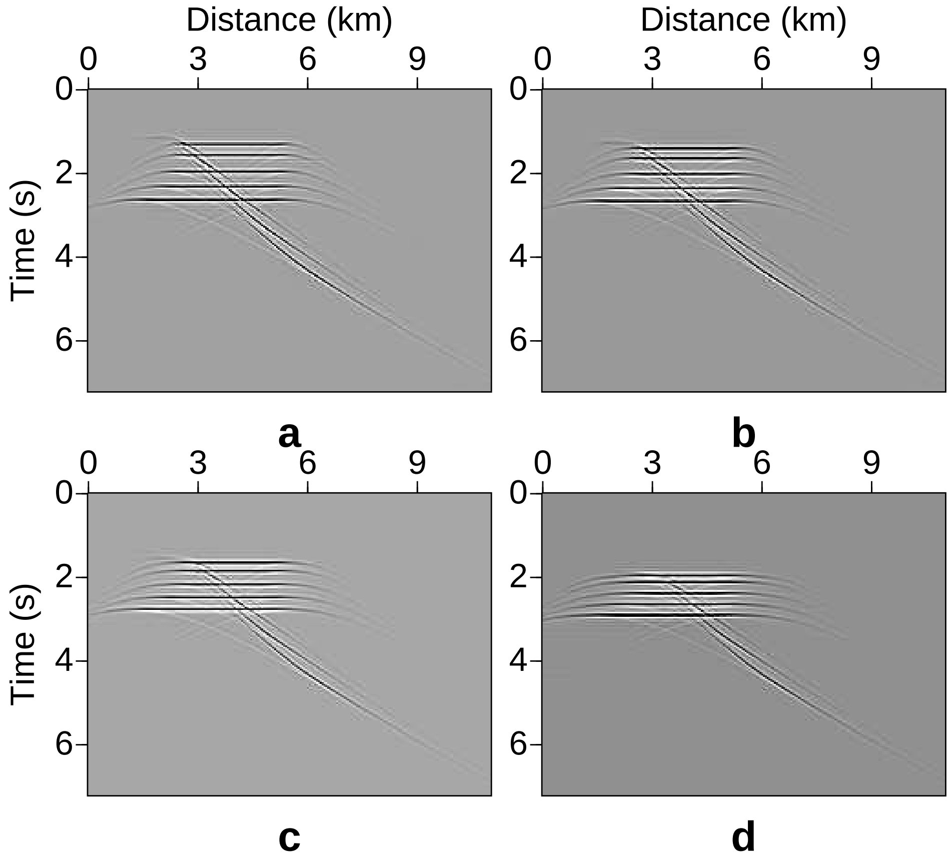

Figure 11: Synthetic seismograms for the model in Figure 10 for (a) coincident source and receiver (zero-offset), (b) an offset of 1 km, (c) an offset of 2 km, and (d) an offset of 3 km. $\boxed{\text{tariq3-synvz}}$ [NR]

of the synthetic data given in Figure 11 plotted in depth for offsets, from top to bottom, of zero, 1, 2, and 3 km, respectively. The migrated sections overall agree well with the model used to generate the synthetic seismograms. However, such an agreement in this $v(z)$ example is less evident compared to what we obtained in the homogeneous medium case. This is some what expected since equivalent medium derivations are approximations. As dip increases slight under migration is apparent, however, these results are preliminary; improvements are expected in a follow up paper.

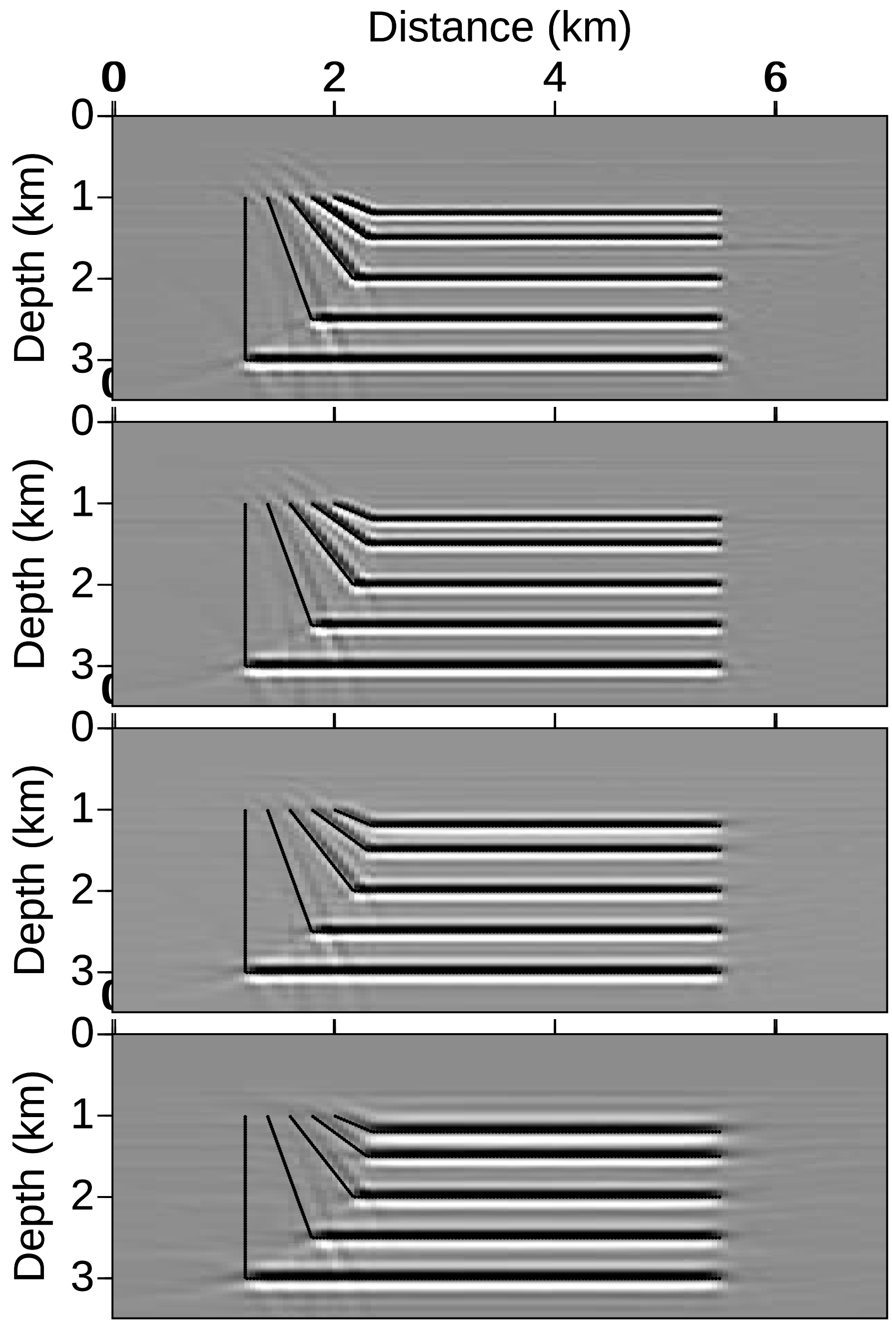

Figure 12: Prestack time migrated sections converted to depth for an offset, from top to bottom, of zero, 1, 2, and 3 km, respectively. The reflector shape in Figure 10 is overlaid on the migration results. tariq3-migvzm [NR]

CONCLUSIONS

The offset-midpoint traveltime equation for transversely isotropic media is derived from its Fourier domain equivalent using the stationary phase method. Perturbation theory and Shank transforms we needed to arrive at a relatively simple analytical form. This Cheop's pyramid equation for VTI media provides accurate traveltimes for practically any strength of anisotropy. It can be used in vertically inhomogeneous media by replacing the medium parameters in the equation by their effective values.

REFERENCES

Alkhalifah, T., and Tsvankin, I., 1995, Velocity analysis for transversely isotropic media: Geophysics, **60**, 1550–1566.

Alkhalifah, T., 1995, Efficient synthetic-seismogram generation in transversely isotropic, inhomogeneous media: Geophysics, **60**, no. 4, 1139–1150.

Alkhalifah, T., 1997a, Acoustic approximations for seismic processing in transversely isotropic media: accepted for Geophysics.

Alkhalifah, T., 1997b, Prestack time migration for anisotropic media: SEP–**94**, 263–298.

Bancroft, J. C., and Geiger, H. D., 1994, Equivalent offset crp gathers: Equivalent offset crp gathers:, 64th Annual Internat. Mtg., Soc. Expl. Geophys., Expanded Abstracts, 672–675.

Banik, N. C., 1984, Velocity anisotropy of shales and depth estimation in the north sea basin: Geophysics, **49**, no. 9, 1411–1419.

Buchanan, J. L., and Turner, P. R., 1978, Numerical methods and analysis: McGraw-Hill, Inc.

Gazdag, J., 1978, Wave equation migration with the phase-shift method: Geophysics, **43**, no. 7, 1342–1351.

Hake, H., Helbig, K., and Mesdag, C. S., 1984, Three-term taylor series for $t^2 - x^2$ curves over layered transversely isotropic ground: Geophys. Prosp., **58**, 1454–1467.

Karrenback, M., and Gardner, G. H. F., 1988, Three-dimensional time slice migration: Three-dimensional time slice migration:, 58th Annual Internat. Mtg., Soc. Expl. Geophys., Expanded Abstracts, Session:S12.7.

Richards, T. C., 1960, Wide-angle reflections and their application to finding limestone structures in the foothills of western canada: Geophysics, **25**, no. 2, 385–407.

Thomsen, L., 1986, Weak elastic anisotropy: Geophysics, **51**, no. 10, 1954–1966.

Tsvankin, I., and Thomsen, L., 1994, Nonhyperbolic reflection moveout in anisotropic media: Geophysics, **59**, no. 8, 1290–1304.

Yilmaz, O., and Claerbout, J. F., 1980, Prestack partial migration: Geophysics, **45**, no. 12, 1753–1779.

Yilmaz, O., 1979, Prestack partial migration: SEP–**18**.

Zauderer, E., 1989, Partial differential equations of applied mathematics: Wiley-Interscience.

APPENDIX A

STATIONARY POINT SOLUTIONS

To evaluate the integrals in equation (7), using the stationary phase method, we need to calculate the maximum of the phase function, which for VTI media is given by

$$T = \frac{1}{2}\left(\sqrt{1 - \frac{(p_x + p_h)^2 v^2}{1 - 2\eta v^2 (p_x + p_h)^2}} + \sqrt{1 - \frac{(p_x - p_h)^2 v^2}{1 - 2\eta v^2 (p_x - p_h)^2}}\right) + 2p_x(x - x_0) + 2p_h h_0. \tag{A-1}$$

Since the relation between the source-receiver rayparameters (p_s and p_g) and the offset-midpoint rayparameters (p_h and p_x) is linear, we can evaluate the stationary points by solving for p_s and p_g instead of p_h and p_x,

$$T = \frac{1}{2}\left(\sqrt{1 - \frac{p_g^2 v^2}{1 - 2\eta v^2 p_g^2}} + \sqrt{1 - \frac{p_s^2 v^2}{1 - 2\eta v^2 p_s^2}}\right) + 2(p_g + p_s)(x - x_0) + 2(p_g - p_s)h_0. \tag{A-2}$$

Setting the derivative of equation A-2 in terms of p_s and p_g to zero provides us with two independent equations that can be solved for p_s and p_g, separately. Physically, this implies that we are solving for the source-to-image-point traveltime and receiver-to-image-point traveltime, separately, which makes complete sense. The p_s and p_g stationary point solutions can be used later to evaluate p_h and p_x.

First, p_s is evaluated by solving

$$\frac{\partial T}{\partial p_s} = \frac{v^2\,\tau\,p_s}{(1 - 2\,v^2\,\eta\,{p_s}^2)^2\,\sqrt{1 - \frac{v^2\,{p_s}^2}{1 - 2\,v^2\,\eta\,{p_s}^2}}} + y_s = 0, \tag{A-3}$$

where $y_s = 2(x - x_0 - h_0)$. Similarly, p_g is evaluated by solving

$$\frac{\partial T}{\partial p_g} = \frac{v^2\,\tau\,p_g}{(1 - 2\,v^2\,\eta\,{p_g}^2)^2\,\sqrt{1 - \frac{v^2\,{p_g}^2}{1 - 2\,v^2\,\eta\,{p_g}^2}}} + y_g = 0, \tag{A-4}$$

where $y_g = 2(x - x_0 + h_0)$. Equation A-4 is similar to equation A-3, with y_s replaced by y_g, and p_s replaced by p_g. Therefore, solving for p_s will yield an equation that can be used to solve for p_g as well.

To remove the square root in equation A-3, I move y_s to the other side of the equation and square both sides. This will allow us to right equation A-2 in a polynomial form as follows,

$$-{y_s}^2 + {p_s}^2 \left(v^4\,\tau^2 + 6\,v^2\,\eta\,{y_s}^2 + v^2\,(1+2\,\eta)\,{y_s}^2\right) + {p_s}^4 \left(-12\,v^4\,\eta^2\,{y_s}^2 - 6\,v^4\,\eta\,(1+2\,\eta)\,{y_s}^2\right) + {p_s}^6 \left(8\,v^6\,\eta^3\,{y_s}^2 + 12\,v^6\,\eta^2\,(1+2\,\eta)\,{y_s}^2\right) - 8\,v^8\,\eta^3\,(1+2\,\eta)\,{p_s}^8\,{y_s}^2 = 0 \tag{A-5}$$

This is a fourth-order polynomial in p_s^2, which can be solved exactly for the four roots in p_s^2. However, these four roots are given by highly complicated equations which include square roots as well as powers of the order $\frac{1}{3}$. Such equations are not useful for practical use. Thus, I elect to use Shanks transform to obtain approximations that are almost exact, yet more useful for practical implementations. Also, since Shanks transform is based on perturbation theory, it will provide us with the desired solution of p_s^2 among the four possible solutions; the solution based on perturbation from an isotropic model.

Using Shanks transform, described in Appendix D, we obtain

$$p_s^2 = \frac{y_s^2\,\left(y_s^6 + 6\,v^2\,y_s^4\,(1-\eta)\,\tau^2 + 3\,v^4\,y_s^2\,(3+4\,\eta)\,\tau^4 + 4\,v^6\,\tau^6\right)}{v^2\,\left(y_s^2 + v^2\,\tau^2\right)\,\left(y_s^6\,(1+2\,\eta) + 2\,v^2\,y_s^4\,(3+5\,\eta)\,\tau^2 + v^4\,y_s^2\,(9+44\,\eta)\,\tau^4 + 4\,v^6\,\tau^6\right)}. \tag{A-6}$$

Again, p_g is given by the same equation but with y_s replaced by y_g.

APPENDIX B

VERTICALLY HETEROGENOUS MEDIA

The same approach used in homogeneous media is followed here. Starting with the phase of exponential for VTI $v(z)$ media which is given by

$$\phi(p_x, p_h, v, eta, X, \tau) = 0.5\Big(\int_0^\tau \Big(\sqrt{1 - \frac{(p_x+p_h)^2 v^2(t)}{1 - 2\eta(t)(p_x+p_h)^2 v^2(t)}} + \sqrt{1 - \frac{(p_x-p_h)^2 v^2(t)}{1 - 2\eta(t)(p_x-p_h)^2 v^2(t)}}\Big)dt + p_h X + 2p_x(x - x_0)\Big). \tag{B-1}$$

Using Taylor series, I expand equation (B-1) around $p_h = 0$ and $p_x = 0$, which corresponds to small offsets and dips. In the Taylor series expansion of equation (B-1), I drop terms beyond the quartic power in p_h and p_x. Thus,

$$\tau + X\,p_h + 2\,(x-x_0)\,p_x - \frac{{p_h}^2\,\int_0^\tau v(t)^2 dt}{2} - \frac{{p_x}^2\,\int_0^\tau v(t)^2 dt}{2} - \frac{{p_h}^4\,\int_0^\tau v(t)^4\,(1+8\,\eta(t))\,dt}{8}$$

$$-\frac{3\,{p_h}^2\,{p_x}^2\,\int_0^\tau v(t)^4\,(1+8\,\eta(t))\,dt}{4}-\frac{{p_x}^4\,\int_0^\tau v(t)^4\,(1+8\,\eta(t))\,dt}{8}=0 \quad \text{(B-2)}$$

As mentioned earlier, the analytical homogeneous-medium equations can be used to calculate traveltimes in vertically inhomogeneous media, granted that the medium parameters are replaced by their equivalent averages in $v(z)$ media. Thus, equation (A-1) becomes

$$T=0.5\left(\sqrt{1-\frac{(p_x+p_h)^2V^2}{1-2\eta_{\text{eff}}V^2(p_x+p_h)^2}}+\sqrt{1-\frac{(p_x-p_h)^2V^2}{1-2\eta_{\text{eff}}V^2(p_x-p_h)^2}}\right)+2p_x(x-x_0)+2p_h h_0. \quad \text{(B-3)}$$

The Taylor series expansion of equation (B-3) around $p_h=0$ and $p_x=0$, with terms beyond the quartic power in p_h and p_x dropped, yields

$$\tau+X\,p_h+2\,(x-x_0)\,p_x-\frac{\tau\,{p_h}^2\,V^2}{2}-\frac{\tau\,{p_x}^2\,V^2}{2}-\frac{\tau\,{p_h}^4\,V^4\,(1+8\,\eta_{\text{eff}})}{8}$$
$$-\frac{3\,\tau\,{p_h}^2\,{p_x}^2\,V^4\,(1+8\,\eta_{\text{eff}})}{4}-\frac{\tau\,{p_x}^4\,V^4\,(1+8\,\eta_{\text{eff}})}{8}=0. \quad \text{(B-4)}$$

Matching coefficients of terms with the same power in p_x and p_h in equations (B-2) and (B-4) provides us with two key relations:

$$V^2(\tau)=\frac{1}{\tau}\int_0^\tau v^2(t)dt, \quad \text{(B-5)}$$

and

$$\eta_{\text{eff}}(\tau)=\frac{1}{8}\{\frac{1}{t_0V^4(\tau)}\int_0^\tau v^4(t)[1+8\eta(t)]dt-1\}. \quad \text{(B-6)}$$

The stationary points (p_h and p_x), in vertically inhomogeneous media, satisfy

$$\frac{\partial\phi}{\partial p_h}=X+\int_0^\tau\Bigg(\frac{(p_x-p_h)v^2(t)}{[1-2\eta(t)p_h^2v^2(t)+4\eta(t)p_hp_xv^2(t)-2\eta(t)p_x^2v^2(t)]^2\sqrt{1-\frac{(p_x-p_h)^2v^2(t)}{1-2\eta(t)v^2(t)(p_x-p_h)^2}}}$$
$$-\frac{(p_x+p_h)v^2(t)}{(1-2\eta(t)v^2(t)p_h^2-4\eta(t)p_hp_xv^2(t)-2\eta(t)p_x^2v^2(t)]^2\sqrt{1-\frac{(p_x+p_h)^2v^2(t)}{1-2\eta(t)v^2(t)(p_x+p_h)^2}}}\Bigg)dt=0 \quad \text{(B-7)}$$

with solutions best solved numerically. Again by expanding this equation in powers of p_x and p_h and matching its coefficients with the coefficients of an equivalent expansion of the effective equation, we obtain equations (B-5) and (B-6) again.

In summary, equations (B-5) and (B-6) provide us with the equivalent relations necessary to use the offset-midpoint traveltime equation for homogeneous VTI media in $v(z)$ media.

APPENDIX C

STATIONARY PHASE APPROXIMATION

The stationary phase method is an approach for solving integrals analytically by evaluating the integrands in regions where they contribute the most. This method is specifically directed to evaluating oscillatory integrands, where the phase function of the integrand is multiplied by a relatively high value. In our case, this value corresponds to the frequency and thus our approximation is asymptotically exact as the frequency approaches ∞.

Integrals of the form

$$I(k) = \int_{-\infty}^{\infty} e^{ik\phi(t)} f(t)\, dt$$

are approximated asymptotically (Zauderer, 1989) when $k \to \infty$ by

$$I(k) \approx e^{ik\phi(t_0)} f(t_0) e^{\mathrm{sign}(\phi''(t_0))\frac{i\pi}{4}} \left[\frac{2\pi}{k \mid \phi''(t_0) \mid}\right]^{\frac{1}{2}} \tag{C-1}$$

where t_0 is the "stationary point" in which the derivative of the phase is zero. The approximation described in equation (C-1) assumes the second derivative is non-zero, which is the case here.

APPENDIX D

SHANKS TRANSFORM

Perturbation theory is based on expressing the solution in terms of power-series expansions of parameters that are expected to be small. Thus, higher power terms have smaller contributions, and as a result, they are usually dropped. The degree of truncation depends on the convergence behavior of the series. I will apply the perturbation theory to evaluate the stationary phase solutions around $\eta = 0$ in VTI media.

Analytical solutions for the quartic equation (A-5) in p_s^2 can be evaluated. They are, however, complicated, and some of them actually do not exist ($\to \infty$) for η=0. Recognizing that η can be small, we develop a perturbation series, that is apply a power-series expansion in terms of η. Unlike weak anisotropy approximations, the resultant solution based on perturbation theory yields good results even for strong anisotropy ($\eta > 0.5$). The key here is to recognize the behavior of the series for large powers of η using Shanks transforms. According to perturbation theory (Buchanan and Turner, 1978), the solution of equation (A-5) can be represented in a power-series expansion in terms of η as follows

$$y = \sum_{i=0}^{\infty} y_i \eta^i, \tag{D-1}$$

where y_i are coefficients of this power series. For practical applications, the power series of equation (D-1) is truncated to n terms as follows

$$A_n = \sum_{i=0}^{n} y_i \eta^i. \tag{D-2}$$

The coefficients, y_i, are determined by inserting the truncated form of equation (D-1) (three terms of the series are enough here) into equation (A-5) and then solving for y_i, recursively. Because η is a variable, we can set the coefficients of each power of η separately to equal zero. This gives a sequence of equations for the y_i expansion coefficients. For example, y_0 is obtained directly from setting η=0, and the result corresponds to the solution for isotropic media. For large η, A_n converges slowly to the exact solution, and, therefore, yields sub-accurate results when used, even if we go up to A_{10}. Truncating after the second term (linear in η, A_1) is referred to as the weak anisotropy approximation. Using Shank transforms (Buchanan and Turner, 1978), one can predict the behavior of the series for large n, and, therefore, eliminate the most pronounced transient behavior of the series (to eliminate the term that has the slowest decay). Following Shanks transform, the solution is evaluated using the following relation

$$y_s = \frac{A_2 A_0 - A_1^2}{A_2 + A_0 - 2A_1}.$$